ChinaCropSM1km: a fine 1km daily Soil Moisture dataset for Crop drylands across China during 1993–2018

Fei Cheng[1], Zhao Zhang[1, 2], Huimin Zhuang[1], Jichong Han[1], Yuchuan Luo[1], Juan Cao[1], Liangliang Zhang[1], Jing Zhang[1], Jialu Xu[1] and Fulu Tao[2, 3, 4]

[1]Academy of Disaster Reduction and Emergency Management Minsitry of Emergency Management & Ministry of Education, School of National Safety and Emergency Management, Beijing Normal University, Beijing 100875, China
[2]Key Laboratory of Land Surface Pattern and Simulation, Institute of Geographical Sciences and Natural Resources Research, Chinese Academy of Sciences, Beijing 100101, China
[3]College of Resources and Environment, University of Chinese Academy of Sciences, Beijing 100049, China
[4]Natural Resources Institute Finland (Luke), FI-00790 Helsinki, Finland

Correspondence to: Zhao Zhang (sunny_zhang@bnu.edu.cn)

Abstract. Soil moisture (SM) is a key variable of regional hydrological cycle and has important applications for water resource and agricultural drought management. Various global soil moisture products have been mostly retrieved from microwave remote sensing data. However, there is currently rare spatially explicit and time-continuous soil moisture information with a high resolution at a nation scale. Here we generated a 1km soil moisture dataset for stable crop drylands in China (ChinaCropSM1km) over 1993−2018 through random forest (RF) algorithm, based on numerous in situ daily observations of soil moisture. We used independently in situ observations (181327 samples) from the Agricultural Meteorological Stations (AMS) across China for training (164202 samples) and others for testing (17125 samples). An irrigation module was firstly developed according to crop type (i.e. wheat, maize), soil depth (0–10 cm, 10–20 cm) and phenology. We produced four daily datasets separately by crop type and soil depth, and their accuracy is all satisfactory (wheat r 0.93, ubRMSE 0.033 m^3m^{-3}; maize r 0.93, ubRMSE 0.035 m^3m^{-3}). The spatio-temporal resolutions and accuracy of ChinaCropSM1km are significantly better than those of global soil moisture products (e.g. r increased by 116 %, ubRMSE decreased by 64 %), including the global remote-sensing-based surface soil moisture dataset (RSSSM) and the European Space Agency (ESA) Climate Change Initiative (CCI) SM. The approach developed in our study could be applied into other regions and crops in the world, and our improved datasets are very valuable for many studies and field managements such as agriculture drought monitoring and crop yield forecasting. The data are published in Zenodo at https://zenodo.org/record/6834530 ($wheat_{0–10}$) (Cheng et al., 2022a), https://zenodo.org/record/6822591 ($wheat_{10–20}$) (Cheng et al., 2022b), https://zenodo.org/record/6822581 ($maize_{0–10}$) (Cheng et al., 2022c) and https://zenodo.org/record/6820166 ($mazie_{10–20}$) (Cheng et al., 2022d).

1 Introduction

Soil moisture (SM) is closely associated with droughts and floods, consequently agricultural productions (Tao et al., 2003). Thus, SM information at a high resolution is critical to improve crop yield prediction (Prasad et al., 2006; Chakrabarti et al., 2014) and drought impact assessment (Sheffield, 2004). However, such higher resolution in both temporal (e.g. daily and more than decade) and spatial scales are still unavailable across China, especially for dry croplands.

SM can be obtained by several ways, including in situ observations (Walker et al., 2004; Bogena et al., 2007), remote sensing retrieval (Mohanty et al., 2017; Wei et al., 2019), and process-based model simulations (Vergopolan et al., 2020; Ahmed et al., 2021). The field observations provide the most accurate SM but being expensive and time-consuming, and large uncertainties from extrapolating the limited observations into larger regions with high heterogeneity (Collow et al., 2012; Crow et al., 2012). The microwave sensors have been applied to retrieve SM in recent years (Schmugge et al., 2002; Wigneron et al., 2003; Amazirh et al., 2018). The microwave sensors can only monitor near-surface SM (0−10 cm) (Eagleman and Lin, 1976; Jackson et al., 1982). The passive microwave sensors can monitor daily SM but with a coarse resolution (25−40 km), comparing with a high spatial resolution (10–30 m) whereas a coarser repetition interval (15−25 days) for active ones (Eagleman and Lin, 1976; Jackson et al., 1982; Mallick et al., 2009). Such SM products have large uncertainties due to the limitations from satellite coverage and downscaling methods, although they can easily cover large regions compared with the in situ observations (Loew et al., 2013; Su et al., 2016; Peng et al., 2017). Deriving the SM from model simulation is also challenging because of its high requirements in input data, computing ability and large uncertainties from model parameters (Wang and Qu, 2009; Yilmaz et al., 2012; Petropoulos et al., 2015). In addition, many studies have found that irrigation, as an additional water supply source other than precipitation, reduces soil albedo (Chen and Dirmeyer, 2019), increases heat capacity (Wang et al., 2019), alters local SM (Lawston et al., 2017), and affects the water/energy budget (Shen et al., 2013). However, few studies have taken irrigation into account in developing SM data products at the national or global scales (Drewniak et al., 2013; Qiu et al., 2016a). Thus, it is critical yet challenging to improve SM accuracy at both spatial and temporal resolutions.

As one part of the Climate Change Initiative (CCI), the European Space Agency (ESA) published a long-term surface SM dataset, and the latest version (v06.1) covered the period of 1978–2020 (https://www.esa-soilmoisture-cci.org/, last access: 10 Apr. 2022) (Dorigo et al., 2017; Gruber et al., 2019; Preimesberger et al., 2021). The ESA CCI SM p*r*oducts are consistent with the observed values at some grassland and farmland sites in China (Liu et al., 2011; Albergel et al., 2013; Dorigo et al., 2015, 2017), however, they have a coarse spatial resolution (~27 km) and lots of coverage gaps (Llamas et al., 2020; Guevara et al., 2021). More recently, based on multiple neural networks, the global remote-sensing-based surface soil moisture (RSSSM) dataset covering 2003–2018 at 0.1° resolution was developed by using Soil Moisture Active Passive (SMAP) SM as the primary training target. RSSSM improved Coefficient of determination (R^2) of 0.46 and Root Mean Squared Error (RMSE) of 0.083 $m^3 m^{-3}$, with a 10-day resolution (Chen et al., 2021). In 2020, another new SM dataset in China from 2002 to 2018 was provided from different passive microwave SM products and model-based downscaling

techniques (Meng et al., 2021). With an improved correlation coefficient (r) of 0.84 and an unbiased root-mean-squared error (ubRMSE) of 0.056 $m^3 m^{-3}$, the new dataset has a 0.05° spatial resolution and a monthly time resolution. These SM products did contribute largely to related agriculture studies and managements, however, they are still too coarse to assess agricultural drought risk and predict crop yield accurately.

Despite numerous efforts have been devoted to develop SM products, major concerns should be addressed: (1) agricultural management activities such as irrigation have not been fully considered by the previous studies, especially in countries like China with extensive areas irrigated (Zhu et al., 2013); (2) both spatial and temporal (e.g. daily) resolutions of SM products need to be improved for regional agricultural managements; (3) the SM accuracy need to be further improved. In recent years, the in situ observations are becoming available (Li et al., 2005). Some new methods such as machine learning are increasingly applied to many fields and have been shown to be robust in incorporating multiple sources data to develop spatiotemporal datasets (Ahmad et al., 2010; Srivastava et al., 2013; Im et al., 2016).

Thus, our main objectives in the study are: to develop a novel method to generate a daily 1km SM dataset for dry croplands across China based on numerous field observations; to evaluate their accuracy and compare them with current products; to explore the spatio-temporal characteristics of soil moisture for crop drylands. We are sure our methods and datasets will be valuable for agriculture drought monitoring and crop yield forecasting.

2 Materials and Method

2.1 Study area

The study area is dominated by dryland crops such as wheat and maize in China, with complex cultivation methods (Wu and Li, 2012) and various irrigation activities (Huang et al., 2015). According to the annual crop harvesting areas of crops across mainland China from 2000 to 2015 (Luo et al., 2020a, b), maize and wheat are the two main crops in China, accounting for 35.4 % of the total harvested area (FAOSTAT, 2019). The study areas and SM in situ field monitoring sites for the two crops are shown in Figure 1.

2.2 Data

2.2.1 In situ SM observations

The in situ SM observation data (http://data.cma.gov.cn/data/detail/dataCode/AGME_AB2_CHN_TEN.html, last access: 18 April 2021) from 1993 to 2018 in this study were obtained from agriculture meteorological sites in China, which recorded the location, crop type, phenology, soil depth and SM. SM was measured at the depths of 10 cm and 20 cm at each agro-meteorological station on the 8th, 18th and 28th of each month. For each sample, crop phenology was observed and recorded by well-trained agricultural technicians in experimental fields (the average field size was 0.15 ha) and then were checked and qualified by the Chinese Agricultural Meteorological Monitoring System (CAMMS). The first layer (0–10 cm) has been

widely used to investigate spatial and temporal characteristics of SM and validate SM retrieved from microwave across China (Lacava et al., 2012; Zeng et al., 2015; Liu et al., 2018; Fang et al., 2020).

We collected the in situ observations of maize (287 sites) and wheat (240 sites), with total 181327 samples (maize: 36226 samples for the 0–10 cm soil layer, 36245 samples for the 10–20 cm soil layer; wheat: 54396 samples for the 0–10 cm soil layer, 54460 samples for the 10–20 cm soil layer).

2.2.2 Environmental factors

The environmental factors are classified into Site features and Gridded features, which both include meteorological data (MD), day of year (DOY), Classified Irrigation (CIR), soil properties (SP), remote sensing data (RSD), and geographical information (GI) (Table 1).

MD includes daily total precipitation (pre) and ante-accumulated precipitation over ten days (pre10) from the meteorological stations across China (CNMSs) (http://data.cma.cn, last access: 10 April 2021) (Figure S1).

CIR was calculated using Eq. (1).

$$\mathrm{CIR} = \begin{cases} 1, C_i P_j D_k SM \geq SMI_{ijk}; \\ 0, C_i P_j D_k SM < SMI_{ijk}; \end{cases} \quad (1)$$

where C_i, P_j, D_k, and SMI_{ijk} are crop type, phenology, soil depth, and the evaluation index of relative soil moisture (SMI) corresponding to the crop type i, phenology j, soil depth k. SMI is a threshold to determine when irrigation is applied (Table 2), which was released by Ministry of Water Resources of China (CNMWR) (http://www.mwr.gov.cn, last access: 10 July 2022) in July 2012.

SP includes sand, silt, gravel, organic carbon, clay contents, soil PH and bulk density, obtained from Harmonized World Soil Database Version 1.2 (http://webarchive.iiasa.ac.at/Research/LUC/External-World-soil-database/HTML/, last access: 18 Aug. 2021). The original 30 arc-second raster spatial resolution data were resampled to a 1 km resolution based on the nearest neighbor interpolation, and the site-related SP were extracted from values to points using ArcGIS 10.5 software (ESRI).

RSD includes Reference Evapotranspiration (pet) and field capacity (fc). pet was obtained from TerraClimate (https://doi.org/10.7923/G43J3B0R, last access: 28 Aug. 2021) which included monthly climate and climatic water balance from 1958-present with a resolution of 1/24° or ~4 km (Abatzoglou et al., 2018). fc was obtained from OpenLandMap (https://zenodo.org/record/2784001, last access: 18 July 2021) (Hengl and Gupta, 2019) which included fc under 33kPa at 0 cm (b0) and 10 cm (b10) depth.

GI includes latitude (lat), longitude (lon), moisture index (im) (Thornthwaite, 1948), and river vector data, provided by the Data Centre for Resources and Environmental Sciences, Chinese Academy of Sciences (http://www.resdc.cn/Default.aspx, accessed on 18 April 2021). The distance from each AMS to river networks at all levels (R4, R5, R12) in China was calculated using Euclidean distance analysis method.

2.2.3 Public SM products for comparison

We used two existing SM products for comparison: 1) The ESA CCI SM data are a merged multi−satellite surface SM product, which consists of active, passive, or combined products. The SM retrievals are from four microwave radiometers (SMMR: Scanning Multichannel Microwave Radiometer, SSM/I: Special Sensor Microwave/Imager, TMI: Tropical Rainfall Measuring Mission (TRMM)'s Microwave Imager, and AMSR-E: Advanced Microwave Scanning Radiometer for the Earth Observing System) and two scatterometers (AMI: Active Microwave Instrument, ASCAT: Advanced Scatterometer) in a 0.25° global daily dataset. The data assimilated relies on their respective sensitivity to vegetation density and uses a Global Land Data Assimilation System (GLDAS) surface SM product (Rodell et al., 2004) as a climatology reference (Wagner et al., 2012). The active/passive products are the integration of the scatterometer /radiometer-based SM retrievals, respectively, while ESA CCI SM product is the fusion of both the active and passive products. We used the v05.2 product for comparison because of its advantages comparing with active/passive products (Liu et al., 2012; Dorigo et al., 2017). 2) The RSSSM is an improved global long-term remote-sensing-based surface SM dataset covering 2003–2018 at 0.1° resolution (https://doi.org/10.1594/PANGAEA.912597). Considering their compatibility, we chose 1995 to 2018 for comparison between ChinaCropSM1km and ESA CCI SM, and the 2003–2018 period for that of ChinaCropSM1km and RSSSM.

2.3 Method

2.3.1 Variable selection and data treatment

For the site-related variables, we use the Extract Values to Points tool to extract the 1km resolution raster information of environmental (i.e. SP, RSD and GI) data to AMS point data, output point data attributes and save it in CSV format to obtain a data set of environmental factors through ArcGIS 10.5, and then we deleted those with high multicollinearity ($|r|> 0.5$) according to the factor stacks (Figure S3 and S4). Thus, the 11 independent variables (pre, pre10, DOY, CIR, T_REF_BULK, R4, im, pet, lat, lon and fc) were selected because they well characterize the impacts of meteorological, temporal, irrigation, soil properties, geographical information on regional SM. We used the "Euclidean distance" option of the Spatial Analyst Tools in ArcGIS10.5 to obtain the variables related with river network in China (Danielsson, 1980). We also applied the kriging interpolation method to obtain precipitation-related variables (e.g. pre and pre10) from CNMSs. Thereafter, all gridded maps were processed in the WGS84 UTM zone 45N Geographic Coordinate System (EPSG:32645), and resampled to the same spatial resolution (1 km).

2.3.2 Model development

Ensemble learning was used to aggregate a collection of algorithms to predict the potential impacts, which represents a better method than that uses any algorithm alone (Brownlee, 2016). Random Forest (RF) is a typical ensemble learning algorithm which can be used to build predictive models for both classification and regression purposes. RF fits an ensemble of models that first train a multitude of decision trees and then obtain predictions by an average or vote through all individual trees

(Breiman, 2001). The algorithm introduces extra randomness when growing trees and searches for the best trees among a random subset of features. This technique results in greater tree diversity, generally yielding an overall better model (Hutengs and Vohland, 2016; Lagomarsino et al., 2017). In addition, bagging method, which constructed multiple training sub-dataset by resampling with replacement of the original dataset, is employed to reduce the variance and overfitting (Díaz-Uriarte and Alvarez de Andrés, 2006; Zhang et al., 2018). Its high accuracy and stability in agricultural fields have been substantiated in several previous studies, especially for predicting grain yield, identifying crop planting areas, and mapping soil properties (Hengl et al., 2015; Jeong et al., 2016; Sun et al., 2019).

Hyper parameters in a RF model are very important to optimize its performance. Such parameters are initially defaulted, and we need investigate their appropriateness or find a potentially better values during developing a RF regression (RFR). The important hyper parameters include follows:

n_estimators: the number of trees that the algorithm builds before taking the maximum voting or average over predictions. A high number of trees increases the performance and makes the predictions more stable, but demand more computations.

max_features: the maximum number of features that the random forest considers on a per-split level. The condition is based on variance for regression.

min_samples_leaf: the minimum number of leafs that are required to split an internal node.

max_samples: ratio of samples needed for training each tree.

We applied the 10-fold cross-validation method to tune the four hyper parameters for avoiding the overfitting of RF models (Figure S5). Meanwhile, we use this 10-fold cross-validation to evaluate model performance (Figure S7).

The detailed irrigation module is shown in Figure S2. Given SM is highly sensitive to irrigation application for crop drylands in China, we firstly used the RF classification (RFC) to build irrigation module. This module aims to predict whether irrigation application occurred there, and assign response variable "1" for irrigation and "0" for without-irrigation according to the response variables and predictor ones (the same environmental indicators used in producing ChinaCropSM1km).

As for the response variable (Classified Irrigation CIR), it is calculated by irrigation threshold (Table 2) and in situ information, including crop type, phenology and soil depth. Then we used the forecasted CIR as an additional predictor, integrating with other key predictor variables, to drive RFR for forecasting SM. Considering the regional differences in SM, we randomly sampled in situ SM observations (90% for training and 10% for testing) in each agricultural zone to develop RF model. Totally, 98576 (65626) and 10820 (6845) observations were used for training and testing the model for wheat (maize), respectively. All these point samples are used to develop pointed-SM model, and then applied these pointed-models developed to inversely calculate the gridded-SM by inputting 1km-raster environmental variables (Figure 2).

The hyper parameters in the optimal model were determined as 50, 1, 1 and 4 for the respective n_estimators, max_samples, min_samples_leaf and max_features according to the highest accuracy during training (Figure S5). We implemented this processes in Matlab9.8.0 (R2020a). More information could be referred to the MATLAB help center (https://www.mathworks.com/help/stats/regressionlearner-app.html, last access: 26 May 2022).

The features importance was evaluated for the RF model with the greatest regression accuracy by ordering the out-of-bag predictor observations, using the Matlab '*oobPermutedPredictorImportance*' function (https://www.mathworks.com/help/stats/regressionbaggedensemble.oobpermutedpredictorimportance.html, last access: 26 May 2022). We also used the method to measure the importance of each predictor variable during predicting ChinaCropSM.

2.3.3 Evaluation metrics for validation and comparison

The in situ observations provide the most accurate SM, all performance measures were calculated using the testing dataset for evaluation purposes. All SM products were evaluated against the in situ observations (testing dataset) according to three metrics: Root Mean Square Error (RMSE; m^3m^{-3}), bias (m^3m^{-3}), unbiased RMSE (ubRMSE; m^3m^{-3}), Explained variance(R^2), and the correlation coefficient (r), which are defined as follows Eqs. (2)–(6):

$$r = \frac{1}{N-1}\sum_{i=1}^{N}\left(\frac{P_i-\overline{P}}{\sigma_P}\right)\left(\frac{O_i-\overline{O}}{\sigma_O}\right) \quad (2)$$

$$R^2 = 1-\frac{\sum_{i=1}^{N}(P_i-O_i)^2}{N\sum_{i=1}^{N}(P_i-\overline{P})} \quad (3)$$

$$bias = \frac{1}{N}\sum_{i=1}^{N}(P_i-O_i) \quad (4)$$

$$RMSE = \sqrt{\frac{1}{N}\sum_{i=1}^{N}(P_i-O_i)^2} \quad (5)$$

$$ubRMSE = \sqrt{RMSE^2-bias^2} \quad (6)$$

where the overbar indicates the mean; P_i is the i^{th} prediction SM from products; O_i is the i^{th} in situ observation SM; N is the total number of observations; and σ_o and σ_p are the standard deviations of the in situ observed or predicted SM, respectively. In addition, we compared our four subset data with RSSSM and ESA CCI SM separately through evaluating their spatial and temporal accuracy related to in situ surface SM observations (Table S1 and S2).

We evaluated our irrigation factor forecasting model results using the receiver operating characteristics (ROC) curve and their Area Under the Curve (AUC) (Table S4) (Fawcett, 2006). Also, we calculated UA (Eq. 7), PA (Eq. 8), and overall accuracy (Eq. 9) based on confusion matrices (Table S3) containing the percentages of the four possible outcomes of a model: True Positive (TP), True Negative (TN), False Positive (FP) and False Negative (FN) (Fawcett, 2006).

$$PA = \frac{TP}{TP+FP} \quad (7)$$

$$UA = \frac{TP}{TP+FN} \quad (8)$$

$$Accuracy = \frac{TP+TN}{TP+FP+TN+FN} \quad (9)$$

3 Results and discussion

3.1 ChinaCropSM1km products validation

The scatterplots between the predicted SM and those observations were displayed by soil layers and crops (Figure 3). We found that the SM predicted by RF model agreed well with in situ SM observations, with ubRMSE of 0.028–0.037, bias of -0.0011–0.0009, *r* from 0.925–0.944. Moreover, the mean bias in predicting SM for wheat was negative (Figure 3-a, b), while those for maize were positive (Figure 3-c, d). These findings suggest that maize SM were overestimated while those for wheat were underestimated. The absolute value of mean bias and RMSE in predicting SM at top soil depth (0–10 cm) for both crops were relative larger (eg. RMSE 0.036>0.028) than that for soil depth of 10–20 cm. It indicates that RF model performed better in predicting the SM content at 10–20 cm layer than that at 0–10 cm layer, which was consistent with the previous studies (O and Orth, 2020).

3.2 The improvement of ChinaCropSM1km products with an irrigation module

Interestingly, all prediction accuracy of SM were consistently improved both for crops and depths (Figure 4) with comparison of those without an irrigation module (Table S5). Specifically, R^2 values were increased by 6.8–9.7%, RMSE were decreased by 16–23% (Table S5). Among these, R^2 values for maize SM were slightly improved than those of wheat and RMSE for maize was decreased more than that of wheat. Such finding further suggests that the irrigation water requirements of maize are higher than for wheat, which was consistent with the reason that summer maize requires large amounts of water to produce high yields. (Mohammed Karrou, 2012).

3.3 The significant scores of different factors for simulating SM

It is critical to select which independent variables involved into a model, neither too many or too less, simultaneously avoiding multicollinearity among them. We have deleted 7 variables due to their high correlations ($|r|> 0.5$) with the 11 variables selected (Figure S3 and S4). Surprisingly, the top first was scored to irrigation factor (CIR), followed by pre10 (ante-accumulated precipitation over ten days) and fc (field capacity) (Figure 5). Current daily precipitation show significantly different importance on SM planted by wheat and maize, with the similarity for DOY. Nevertheless, all other factors show less importance on SM simulation. Comparing with the significant roles of precipitation-related variables (e.g. pre10, pre) on SM in most rainfall-fed areas, however, irrigation shows overwhelming impacts on dryland soil moisture across China (Qiu et al., 2016b). Such result highlights more accurately monitoring management activities, including irrigating times, areas and quantity, will further improve irrigation module, consequently improve SM simulation (Wu et al., 2020; Zhang et al., 2015, 2022).

3.4 The temporal and spatial patterns between ChinaCropSM1km and the in situ SM observations

The SM values in ChinaCropSM1km are significantly correlated with the in situ SM observations, with a mean r of 0.92, 0.94, 0.93 and 0.94, respectively, for wheat$_{0–10}$, wheat$_{10–20}$, maize$_{0–10}$ and maize$_{10–20}$, during the whole growing period (Figure 6). The spatial coefficients for wheat at 10−20 cm are generally higher than the surface SM (0.94 vs. 0.92), and the two soil depths SM in April and September are significantly higher (Figure 6–a, b). We attributed the high spatial correlations of surface SM to irrigation impacts, because April and September are planting time for both spring and winter wheat. The better relationships further substantiated the irrigation module developed in our SM model improves the simulation accuracy for surface SM. Consistently, the spatial coefficients for maize at 10–20cm depth are higher than those for 0−10cm (0.94 vs. 0.93) (Figure7-c, d). At the sowing (Apr.), heading (Jul.), and milking (Aug.) stages, maize usually demanded water supplying a lot. The spatial coefficient for maize SM at both soil depth from May to Aug. were lower than the mean value potentially due to the lack of irrigation applications (Yin et al., 2016) (Figure 6).

We still further analyzed the temporal pattern of SM accuracy in different regions (Figure 7). The median of r values for Huang–Huai–Hai Plain and Northern Arid and Semiarid region were higher than that in other agricultural regions because of larger training samples. Our findings further substantiated that a larger training sample size will cause a higher temporal accuracy, indicated by a higher r and a lower RMSE (Figure S6). However, the poor performance in Yunnan–Guizhou Plateau might be caused by smaller training samples (Figure S6).

3.5 Comparisons between ChinaCropSM1km and public global SM products

We further compared our ChinaCropSM1km with the two popular products through evaluating their spatial-temporal accuracy related to in situ surface SM observations. We summarized their evaluation indexes by individual product in Table 3, which indicated consistently the bolds for our ChinaCropSM1km (all r >0.90, RMSE <0.04), while RSSSM and ESA CCI SM were shown by r <0.50 and RMSE >0.1.

To match the different spatial resolutions of three products, we calculated the averages of all in-site observations in the same pixel (e.g. 1 km, 27 km or 0.1°) to make their spatial-temporal accuracy comparable. Interestingly, all indexes of our products were consistently indicated by the higher accuracy (e.g. r 0.94, bias 0.005, RMSE 0.034, ubRMSE 0.034) (Figure 9). RSSSM dataset significantly underestimated SM with an averaged bias of −0.114, companying with a higher RMSE of 0.150. ESA CCI SM performed better than RSSSM (e.g. RMSE 0.11 vs. 0.15) derived from Soil Moisture Active Passive (SMAP) (Entekhabi et al., 2010), and we ascribed such improvement partly into some corrections based on in situ observations for ESA CCI SM (Dorigo et al., 2017). Such results highlight SM products derived solely from remote sensing satellites should be corrected with ground observations. Moreover, neither RSSSM nor ESA CCI SM had considered the irrigation activities, thus their spatial correlations with ground observes are incomparable to those of our products (r 0.944 vs. 0.381 0.256) (Figure 8). Our study substantiates strongly that an irrigation module should be taken into account when developing SM simulation models of producing SM products.

4 Data availability

The 1km gridded daily Soil Moisture for Croplands in China (ChinaCropSM1km) is available at https://zenodo.org/record/6834530 ($wheat_{0–10}$) (Cheng et al., 2022a), https://zenodo.org/record/6822591 ($wheat_{10–20}$) (Cheng et al., 2022b), https://zenodo.org/record/6822581 ($maize_{0–10}$) (Cheng et al., 2022c) and https://zenodo.org/record/6820166 ($mazie_{10–20}$) (Cheng et al., 2022d).

5 Discussion and Conclusions

We developed a daily 1km soil moisture dataset based on numerous field observations (181327 samples) from 1993–2018, which significantly enrich the current SM datasets available. Our ChinaCropSM1km shows higher temporal-spatial resolution and accuracy than the popular global SM products. Moreover, to date, few studies have provided a daily SM product with such higher resolution, combining different soil depths and an irrigation module. ChinaCropSM1km is the first SM product with a higher spatial resolution (~1km) at 0–10, 10–20 cm depth in China croplands by compiling the ground observations and using RF method.

Our ChinaCropSM1km predicted by RF model agreed well with in situ SM observations (ubRMSE ranges from 0.028–0.037, bias ranges from −0.0011–0.0009, r ranges from 0.925–0.944, and R^2 ranges from 0.860–0.895). An irrigation module was firstly developed according to crop type (i.e. wheat, maize), soil depth (0–10 cm, 10–20 cm) and phenology. All prediction accuracy of SM were consistently improved (R^2 values were increased by 6.8~9.7%, RMSE were decreased by 16~23%) both for crops and depths. Meanwhile, ChinaCropSM1km generally has advantages over other popular gridded SM products (RSSSM and ESA CCI SM) through evaluating their spatial-temporal accuracy related to in situ SM as the benchmark. Our ChinaCropSM1km has relatively higher accuracy (all r >0.90, RMSE <0.04), while RSSSM and ESA CCI SM were shown by r <0.50 and RMSE >0.1.

The ChinaCropSM dataset are credible and accurate according to the results comparing with the public datasets, however, some limitations are still existed in our study. First, the limited AMS irrigation records may lead to the uncertainty in the irrigation factor predictions. More detailed irrigation information will help to improve irrigation module performances. Second, our method for generating cropland SM is applicable to other regions and crops, but more environmental variables will be increasingly required considering the SM variabilities are complex processes controlled by many factors (Famiglietti et al., 2008; Qin et al., 2013; Guevara and Vargas, 2019), especially for irrigation activities. For example, to characterize more accurately the irrigation activities, many field samples are highly required in both spatial and temporal resolutions. Other auxiliary data on information of crop growth, classification, and managements (e.g. irrigation frequency, amount and method) will benefit to develop our irrigation module and derive SM datasets more accurately. Third, different splitting methods during training and testing do affect model performance. Selecting which splitting method to improve the generalization performance is dependent on data. Generally, the larger size of data, the smaller effect of the splitting methods on the results (Birba, 2020). Moreover, advanced algorithms will be potential alternatives for random forest due to its strong

dependence on inputs (Breiman, 2001; Rasmussen, 2004). Improving irrigation module should be focused on details such as irrigation amount and frequency, which will significantly help to verify and improve the accuracy of both irrigation and SM predictions. We are sure more accurate SM dataset will be produced by applying the approach into other crops and areas in future with all above improvements.

Author contributions

FC, HZ, ZZ, JH, JC, YL, LZ, JZ and JX contributed to the design of this research; FC and ZZ collectively prepared the manuscript with contributions from all co-authors; JH, JC, YL, LZ, JX and JZ revised the manuscript; FC and HZ developed the model code.

Competing interests

The authors declare that they have no conflict of interest.

Financial support

This study was supported by the National Key Research and Development Program of China (grant no. 2020YFA0608201) and the National Natural Science Foundation of China (grant no. 41977405).

References

Abatzoglou, J. T., Dobrowski, S. Z., Parks, S. A., and Hegewisch, K. C.: TerraClimate, a high-resolution global dataset of monthly climate and climatic water balance from 1958–2015, Sci Data, 5, 170191, https://doi.org/10.1038/sdata.2017.191, 2018.

Ahmad, S., Kalra, A., and Stephen, H.: Estimating soil moisture using remote sensing data: A machine learning approach, Advances in Water Resources, 33, 69–80, https://doi.org/10.1016/j.advwatres.2009.10.008, 2010.

Ahmed, A. A. M., Deo, R. C., Raj, N., Ghahramani, A., Feng, Q., Yin, Z., and Yang, L.: Deep Learning Forecasts of Soil Moisture: Convolutional Neural Network and Gated Recurrent Unit Models Coupled with Satellite-Derived MODIS, Observations and Synoptic-Scale Climate Index Data, Remote Sensing, 13, 554, https://doi.org/10.3390/rs13040554, 2021.

Albergel, C., Dorigo, W., Reichle, R. H., Balsamo, G., de Rosnay, P., Muñoz-Sabater, J., Isaksen, L., de Jeu, R., and Wagner, W.: Skill and Global Trend Analysis of Soil Moisture from Reanalyses and Microwave Remote Sensing, Journal of Hydrometeorology, 14, 1259–1277, https://doi.org/10.1175/JHM-D-12-0161.1, 2013.

Amazirh, A., Merlin, O., Er-Raki, S., Gao, Q., Rivalland, V., Malbeteau, Y., Khabba, S., and Escorihuela, M. J.: Retrieving surface soil moisture at high spatio-temporal resolution from a synergy between Sentinel-1 radar and Landsat thermal data: A study case over bare soil, Remote Sensing of Environment, 211, 321–337, https://doi.org/10.1016/j.rse.2018.04.013, 2018.

Birba, D. E.: A Comparative study of data splitting algorithms for machine learning model selection, 2020.

Bogena, H. R., Huisman, J. A., Oberdörster, C., and Vereecken, H.: Evaluation of a low-cost soil water content sensor for wireless network applications, Journal of Hydrology, 344, 32–42, https://doi.org/10.1016/j.jhydrol.2007.06.032, 2007.

Breiman, L.: Random forests, Machine learning, 45, 5–32, 2001.

Brownlee, J.: Machine learning mastery with python, Machine Learning Mastery Pty Ltd, 527, 100–120, 2016.

Chakrabarti, S., Bongiovanni, T., Judge, J., Zotarelli, L., and Bayer, C.: Assimilation of SMOS Soil Moisture for Quantifying Drought Impacts on Crop Yield in Agricultural Regions, IEEE J. Sel. Top. Appl. Earth Observations Remote Sensing, 7, 3867–3879, https://doi.org/10.1109/JSTARS.2014.2315999, 2014.

Chen, L. and Dirmeyer, P. A.: Global observed and modelled impacts of irrigation on surface temperature, Int J Climatol, 39, 2587–2600, https://doi.org/10.1002/joc.5973, 2019.

Chen, Y., Feng, X., and Fu, B.: An improved global remote-sensing-based surface soil moisture (RSSSM) dataset covering 2003–2018, Earth Syst. Sci. Data, 13, 1–31, https://doi.org/10.5194/essd-13-1-2021, 2021.

Cheng, F., Zhang, Z., Zhuang, H., Han, J., Luo, Y., Cao, J., Zhang, L., Zhang, J., Tao, F., and Xu, J.: ChinaCropSM1km: a fine 1km daily Soil Moisture dataset for Crop drylands across China during 1993–2018, https://doi.org/10.5281/ZENODO.6834530, 2022a.

Cheng, F., Zhang, Z., Zhuang, H., Han, J., Luo, Y., Cao, J., Zhang, L., Zhang, J., Tao, F., and Xu, J.: ChinaCropSM1km: a fine 1km daily Soil Moisture dataset for Crop drylands across China during 1993–2018, https://doi.org/10.5281/ZENODO.6822591, 2022b.

Cheng, F., Zhang, Z., Zhuang, H., Han, J., Luo, Y., Cao, J., Zhang, L., Zhang, J., Tao, F., and Xu, J.: ChinaCropSM1km: a fine 1km daily Soil Moisture dataset for Crop drylands across China during 1993–2018, https://doi.org/10.5281/ZENODO.6822581, 2022c.

Cheng, F., Zhang, Z., Zhuang, H., Han, J., Luo, Y., Cao, J., Zhang, L., Zhang, J., Tao, F., and Xu, J.: ChinaCropSM1km: a fine 1km daily Soil Moisture dataset for Crop drylands across China during 1993–2018, https://doi.org/10.5281/ZENODO.6820166, 2022d.

Collow, T. W., Robock, A., Basara, J. B., and Illston, B. G.: Evaluation of SMOS retrievals of soil moisture over the central United States with currently available in situ observations: EVALUATION OF SMOS WITH IN SITU DATA, J. Geophys. Res., 117, n/a-n/a, https://doi.org/10.1029/2011JD017095, 2012.

Crow, W. T., Berg, A. A., Cosh, M. H., Loew, A., Mohanty, B. P., Panciera, R., de Rosnay, P., Ryu, D., and Walker, J. P.: Upscaling sparse ground-based soil moisture observations for the validation of coarse-resolution satellite soil moisture products: UPSCALING SOIL MOISTURE, Rev. Geophys., 50, https://doi.org/10.1029/2011RG000372, 2012.

Danielsson, P.-E.: Euclidean distance mapping, Computer Graphics and Image Processing, 14, 227–248, https://doi.org/10.1016/0146-664X(80)90054-4, 1980.

Díaz-Uriarte, R. and Alvarez de Andrés, S.: Gene selection and classification of microarray data using random forest, BMC Bioinformatics, 7, 3, https://doi.org/10.1186/1471-2105-7-3, 2006.

Dorigo, W., Wagner, W., Albergel, C., Albrecht, F., Balsamo, G., Brocca, L., Chung, D., Ertl, M., Forkel, M., Gruber, A., Haas, E., Hamer, P. D., Hirschi, M., Ikonen, J., de Jeu, R., Kidd, R., Lahoz, W., Liu, Y. Y., Miralles, D., Mistelbauer, T., Nicolai-Shaw, N., Parinussa, R., Pratola, C., Reimer, C., van der Schalie, R., Seneviratne, S. I., Smolander, T., and Lecomte, P.: ESA CCI Soil Moisture for improved Earth system understanding: State-of-the art and future directions, Remote Sensing of Environment, 203, 185–215, https://doi.org/10.1016/j.rse.2017.07.001, 2017.

Dorigo, W. A., Gruber, A., De Jeu, R. A. M., Wagner, W., Stacke, T., Loew, A., Albergel, C., Brocca, L., Chung, D., Parinussa, R. M., and Kidd, R.: Evaluation of the ESA CCI soil moisture product using ground-based observations, Remote Sensing of Environment, 162, 380–395, https://doi.org/10.1016/j.rse.2014.07.023, 2015.

Drewniak, B., Song, J., Prell, J., Kotamarthi, V. R., and Jacob, R.: Modeling agriculture in the Community Land Model, Geosci. Model Dev., 6, 495–515, https://doi.org/10.5194/gmd-6-495-2013, 2013.

Eagleman, J. R. and Lin, W. C.: Remote sensing of soil moisture by a 21-cm passive radiometer, J. Geophys. Res., 81, 3660–3666, https://doi.org/10.1029/JC081i021p03660, 1976.

Entekhabi, D., Njoku, E. G., O'Neill, P. E., Kellogg, K. H., Crow, W. T., Edelstein, W. N., Entin, J. K., Goodman, S. D., Jackson, T. J., Johnson, J., Kimball, J., Piepmeier, J. R., Koster, R. D., Martin, N., McDonald, K. C., Moghaddam, M., Moran, S., Reichle, R., Shi, J. C., Spencer, M. W., Thurman, S. W., Tsang, L., and Van Zyl, J.: The Soil Moisture Active Passive (SMAP) Mission, Proc. IEEE, 98, 704–716, https://doi.org/10.1109/JPROC.2010.2043918, 2010.

Famiglietti, J. S., Ryu, D., Berg, A. A., Rodell, M., and Jackson, T. J.: Field observations of soil moisture variability across scales: SOIL MOISTURE VARIABILITY ACROSS SCALES, Water Resour. Res., 44, https://doi.org/10.1029/2006WR005804, 2008.

Fang, B., Lakshmi, V., Bindlish, R., Jackson, T. J., and Liu, P.-W.: Evaluation and validation of a high spatial resolution satellite soil moisture product over the Continental United States, Journal of Hydrology, 588, 125043, https://doi.org/10.1016/j.jhydrol.2020.125043, 2020.

Fawcett, T.: An introduction to ROC analysis, Pattern Recognition Letters, 27, 861–874, https://doi.org/10.1016/j.patrec.2005.10.010, 2006.

FAOSTAT (Food and Agriculture Organization Corporate Statistical Database): FAO online database, available at: http://www.fao.org/faostat/en/#data/QCL (last access: October 2021), 2019, Crops and livestock products.

Gruber, A., Scanlon, T., van der Schalie, R., Wagner, W., and Dorigo, W.: Evolution of the ESA CCI Soil Moisture climate data records and their underlying merging methodology, Earth Syst. Sci. Data, 11, 717–739, https://doi.org/10.5194/essd-11-717-2019, 2019.

Guevara, M. and Vargas, R.: Downscaling satellite soil moisture using geomorphometry and machine learning, PLoS ONE, 14, e0219639, https://doi.org/10.1371/journal.pone.0219639, 2019.

Guevara, M., Taufer, M., and Vargas, R.: Gap-free global annual soil moisture: 15 km grids for 1991–2018, Earth Syst. Sci. Data, 13, 1711–1735, https://doi.org/10.5194/essd-13-1711-2021, 2021.

Hengl, T. and Gupta, S.: Soil water content (volumetric %) for 33kPa and 1500kPa suctions predicted at 6 standard depths (0, 10, 30, 60, 100 and 200 cm) at 250 m resolution (v0.1), https://doi.org/10.5281/ZENODO.2629589, 2019.

Hengl, T., Heuvelink, G. B. M., Kempen, B., Leenaars, J. G. B., Walsh, M. G., Shepherd, K. D., Sila, A., MacMillan, R. A., Mendes de Jesus, J., Tamene, L., and Tondoh, J. E.: Mapping Soil Properties of Africa at 250 m Resolution: Random Forests Significantly Improve Current Predictions, PLoS ONE, 10, e0125814, https://doi.org/10.1371/journal.pone.0125814, 2015.

Huang, S., Krysanova, V., Zhai, J., and Su, B.: Impact of Intensive Irrigation Activities on River Discharge Under Agricultural Scenarios in the Semi-Arid Aksu River Basin, Northwest China, Water Resour Manage, 29, 945–959, https://doi.org/10.1007/s11269-014-0853-2, 2015.

Hutengs, C. and Vohland, M.: Downscaling land surface temperatures at regional scales with random forest regression, Remote Sensing of Environment, 178, 127–141, https://doi.org/10.1016/j.rse.2016.03.006, 2016.

Im, J., Park, S., Rhee, J., Baik, J., and Choi, M.: Downscaling of AMSR-E soil moisture with MODIS products using machine learning approaches, Environ Earth Sci, 75, 1120, https://doi.org/10.1007/s12665-016-5917-6, 2016.

Jackson, T. J., Schmugge, T. J., and Wang, J. R.: Passive microwave sensing of soil moisture under vegetation canopies, Water Resour. Res., 18, 1137–1142, https://doi.org/10.1029/WR018i004p01137, 1982.

Jeong, J. H., Resop, J. P., Mueller, N. D., Fleisher, D. H., Yun, K., Butler, E. E., Timlin, D. J., Shim, K.-M., Gerber, J. S., Reddy, V. R., and Kim, S.-H.: Random Forests for Global and Regional Crop Yield Predictions, PLoS ONE, 11, e0156571, https://doi.org/10.1371/journal.pone.0156571, 2016.

Lacava, T., Matgen, P., Brocca, L., Bittelli, M., Pergola, N., Moramarco, T., and Tramutoli, V.: A First Assessment of the SMOS Soil Moisture Product With In Situ and Modeled Data in Italy and Luxembourg, IEEE Trans. Geosci. Remote Sensing, 50, 1612–1622, https://doi.org/10.1109/TGRS.2012.2186819, 2012.

Lagomarsino, D., Tofani, V., Segoni, S., Catani, F., and Casagli, N.: A Tool for Classification and Regression Using Random Forest Methodology: Applications to Landslide Susceptibility Mapping and Soil Thickness Modeling, Environ Model Assess, 22, 201–214, https://doi.org/10.1007/s10666-016-9538-y, 2017.

Lawston, P. M., Santanello, J. A., and Kumar, S. V.: Irrigation Signals Detected From SMAP Soil Moisture Retrievals: Irrigation Signals Detected From SMAP, Geophys. Res. Lett., 44, 11,860-11,867, https://doi.org/10.1002/2017GL075733, 2017.

Li, H., Robock, A., Liu, S., Mo, X., and Viterbo, P.: Evaluation of Reanalysis Soil Moisture Simulations Using Updated Chinese Soil Moisture Observations, Journal of Hydrometeorology, 6, 180–193, https://doi.org/10.1175/JHM416.1, 2005.

Liu, Y., Yang, Y., and Yue, X.: Evaluation of Satellite-Based Soil Moisture Products over Four Different Continental In-Situ Measurements, Remote Sensing, 10, 1161, https://doi.org/10.3390/rs10071161, 2018.

Liu, Y. Y., Parinussa, R. M., Dorigo, W. A., De Jeu, R. A. M., Wagner, W., van Dijk, A. I. J. M., McCabe, M. F., and Evans, J. P.: Developing an improved soil moisture dataset by blending passive and active microwave satellite-based retrievals, Hydrol. Earth Syst. Sci., 15, 425–436, https://doi.org/10.5194/hess-15-425-2011, 2011.

Liu, Y. Y., Dorigo, W. A., Parinussa, R. M., de Jeu, R. A. M., Wagner, W., McCabe, M. F., Evans, J. P., and van Dijk, A. I. J. M.: Trend-preserving blending of passive and active microwave soil moisture retrievals, Remote Sensing of Environment, 123, 280–297, https://doi.org/10.1016/j.rse.2012.03.014, 2012.

Llamas, R. M., Guevara, M., Rorabaugh, D., Taufer, M., and Vargas, R.: Spatial Gap-Filling of ESA CCI Satellite-Derived Soil Moisture Based on Geostatistical Techniques and Multiple Regression, Remote Sensing, 12, 665, https://doi.org/10.3390/rs12040665, 2020.

Loew, A., Stacke, T., Dorigo, W., de Jeu, R., and Hagemann, S.: Potential and limitations of multidecadal satellite soil moisture observations for selected climate model evaluation studies, Hydrol. Earth Syst. Sci., 17, 3523–3542, https://doi.org/10.5194/hess-17-3523-2013, 2013.

Luo, Y., Zhang, Z., Chen, Y., Li, Z., and Tao, F.: ChinaCropPhen1km: a high-resolution crop phenological dataset for three staple crops in China during 2000–2015 based on leaf area index (LAI) products, Earth Syst. Sci. Data, 12, 197–214, https://doi.org/10.5194/essd-12-197-2020, 2020a.

Luo, Y., Zhang, Z., Li, Z., Chen, Y., Zhang, L., Cao, J., and Tao, F.: Identifying the spatiotemporal changes of annual harvesting areas for three staple crops in China by integrating multi-data sources, Environ. Res. Lett., 15, 074003, https://doi.org/10.1088/1748-9326/ab80f0, 2020b.

Mallick, K., Bhattacharya, B. K., and Patel, N. K.: Estimating volumetric surface moisture content for cropped soils using a soil wetness index based on surface temperature and NDVI, Agricultural and Forest Meteorology, 149, 1327–1342, https://doi.org/10.1016/j.agrformet.2009.03.004, 2009.

Meng, X., Mao, K., Meng, F., Shi, J., Zeng, J., Shen, X., Cui, Y., Jiang, L., and Guo, Z.: A fine-resolution soil moisture dataset for China in 2002–2018, Earth Syst. Sci. Data, 13, 3239–3261, https://doi.org/10.5194/essd-13-3239-2021, 2021.

Mohammed Karrou: Yield and water productivity of maize and wheat under deficit and raised bed irrigation practices in Egypt, Afr. J. Agric. Res., 7, https://doi.org/10.5897/AJAR11.2109, 2012.

Mohanty, B. P., Cosh, M. H., Lakshmi, V., and Montzka, C.: Soil Moisture Remote Sensing: State-of-the-Science, Vadose Zone Journal, 16, vzj2016.10.0105, https://doi.org/10.2136/vzj2016.10.0105, 2017.

O, S. and Orth, R.: Global soil moisture from in-situ measurements using machine learning -- SoMo.ml, http://arxiv.org/abs/2010.02374, 5 October 2020.

Peng, J., Loew, A., Merlin, O., and Verhoest, N. E. C.: A review of spatial downscaling of satellite remotely sensed soil moisture: Downscale Satellite-Based Soil Moisture, Rev. Geophys., 55, 341–366, https://doi.org/10.1002/2016RG000543, 2017.

Petropoulos, G. P., Ireland, G., and Barrett, B.: Surface soil moisture retrievals from remote sensing: Current status, products & future trends, Physics and Chemistry of the Earth, Parts A/B/C, 83–84, 36–56, https://doi.org/10.1016/j.pce.2015.02.009, 2015.

Prasad, A. K., Chai, L., Singh, R. P., and Kafatos, M.: Crop yield estimation model for Iowa using remote sensing and surface parameters, International Journal of Applied Earth Observation and Geoinformation, 8, 26–33, https://doi.org/10.1016/j.jag.2005.06.002, 2006.

Preimesberger, W., Scanlon, T., Su, C.-H., Gruber, A., and Dorigo, W.: Homogenization of Structural Breaks in the Global ESA CCI Soil Moisture Multisatellite Climate Data Record, IEEE Trans. Geosci. Remote Sensing, 59, 2845–2862, https://doi.org/10.1109/TGRS.2020.3012896, 2021.

Qin, J., Yang, K., Lu, N., Chen, Y., Zhao, L., and Han, M.: Spatial upscaling of in-situ soil moisture measurements based on MODIS-derived apparent thermal inertia, Remote Sensing of Environment, 138, 1–9, https://doi.org/10.1016/j.rse.2013.07.003, 2013.

Qiu, J., Gao, Q., Wang, S., and Su, Z.: Comparison of temporal trends from multiple soil moisture data sets and precipitation: The implication of irrigation on regional soil moisture trend, International Journal of Applied Earth Observation and Geoinformation, 48, 17–27, https://doi.org/10.1016/j.jag.2015.11.012, 2016a.

Qiu, J., Gao, Q., Wang, S., and Su, Z.: Comparison of temporal trends from multiple soil moisture data sets and precipitation: The implication of irrigation on regional soil moisture trend, International Journal of Applied Earth Observation and Geoinformation, 48, 17–27, https://doi.org/10.1016/j.jag.2015.11.012, 2016b.

Rasmussen, C. E.: Gaussian Processes in Machine Learning, in: Advanced Lectures on Machine Learning, vol. 3176, edited by: Bousquet, O., von Luxburg, U., and Rätsch, G., Springer Berlin Heidelberg, Berlin, Heidelberg, 63–71, https://doi.org/10.1007/978-3-540-28650-9_4, 2004.

Rodell, M., Houser, P. R., Jambor, U., Gottschalck, J., Mitchell, K., Meng, C.-J., Arsenault, K., Cosgrove, B., Radakovich, J., Bosilovich, M., Entin, J. K., Walker, J. P., Lohmann, D., and Toll, D.: The Global Land Data Assimilation System, Bull. Amer. Meteor. Soc., 85, 381–394, https://doi.org/10.1175/BAMS-85-3-381, 2004.

Schmugge, T. J., Kustas, W. P., Ritchie, J. C., Jackson, T. J., and Rango, A.: Remote sensing in hydrology, Advances in Water Resources, 25, 1367–1385, https://doi.org/10.1016/S0309-1708(02)00065-9, 2002.

Sheffield, J.: A simulated soil moisture based drought analysis for the United States, J. Geophys. Res., 109, D24108, https://doi.org/10.1029/2004JD005182, 2004.

Shen, Y., Zhang, Y., R. Scanlon, B., Lei, H., Yang, D., and Yang, F.: Energy/water budgets and productivity of the typical croplands irrigated with groundwater and surface water in the North China Plain, Agricultural and Forest Meteorology, 181, 133–142, https://doi.org/10.1016/j.agrformet.2013.07.013, 2013.

Srivastava, P. K., Han, D., Ramirez, M. R., and Islam, T.: Machine Learning Techniques for Downscaling SMOS Satellite Soil Moisture Using MODIS Land Surface Temperature for Hydrological Application, Water Resour Manage, 27, 3127–3144, https://doi.org/10.1007/s11269-013-0337-9, 2013.

Su, C.-H., Zhang, J., Gruber, A., Parinussa, R., Ryu, D., Crow, W. T., and Wagner, W.: Error decomposition of nine passive and active microwave satellite soil moisture data sets over Australia, Remote Sensing of Environment, 182, 128–140, https://doi.org/10.1016/j.rse.2016.05.008, 2016.

Sun, C., Bian, Y., Zhou, T., and Pan, J.: Using of Multi-Source and Multi-Temporal Remote Sensing Data Improves Crop-Type Mapping in the Subtropical Agriculture Region, Sensors, 19, 2401, https://doi.org/10.3390/s19102401, 2019.

Tao, F., Yokozawa, M., Hayashi, Y., and Lin, E.: Changes in agricultural water demands and soil moisture in China over the last half-century and their effects on agricultural production, Agricultural and Forest Meteorology, 118, 251–261, https://doi.org/10.1016/S0168-1923(03)00107-2, 2003.

Thornthwaite, C. W.: An Approach toward a Rational Classification of Climate, Geographical Review, 38, 55, https://doi.org/10.2307/210739, 1948.

Vergopolan, N., Chaney, N. W., Beck, H. E., Pan, M., Sheffield, J., Chan, S., and Wood, E. F.: Combining hyper-resolution land surface modeling with SMAP brightness temperatures to obtain 30-m soil moisture estimates, Remote Sensing of Environment, 242, 111740, https://doi.org/10.1016/j.rse.2020.111740, 2020.

Wagner, W., Dorigo, W., de Jeu, R., Fernandez, D., Benveniste, J., Haas, E., and Ertl, M.: FUSION OF ACTIVE AND PASSIVE MICROWAVE OBSERVATIONS TO CREATE AN ESSENTIAL CLIMATE VARIABLE DATA RECORD ON SOIL MOISTURE, ISPRS Ann. Photogramm. Remote Sens. Spatial Inf. Sci., I–7, 315–321, https://doi.org/10.5194/isprsannals-I-7-315-2012, 2012.

Walker, J. P., Willgoose, G. R., and Kalma, J. D.: In situ measurement of soil moisture: a comparison of techniques, Journal of Hydrology, 293, 85–99, https://doi.org/10.1016/j.jhydrol.2004.01.008, 2004.

Wang, C., Wang, Z.-H., and Yang, J.: Urban water capacity: Irrigation for heat mitigation, Computers, Environment and Urban Systems, 78, 101397, https://doi.org/10.1016/j.compenvurbsys.2019.101397, 2019.

Wang, L. and Qu, J. J.: Satellite remote sensing applications for surface soil moisture monitoring: A review, Front. Earth Sci. China, 3, 237–247, https://doi.org/10.1007/s11707-009-0023-7, 2009.

Wei, Z., Meng, Y., Zhang, W., Peng, J., and Meng, L.: Downscaling SMAP soil moisture estimation with gradient boosting decision tree regression over the Tibetan Plateau, Remote Sensing of Environment, 225, 30–44, https://doi.org/10.1016/j.rse.2019.02.022, 2019.

Wigneron, J.-P., Calvet, J.-C., Pellarin, T., Van de Griend, A. A., Berger, M., and Ferrazzoli, P.: Retrieving near-surface soil moisture from microwave radiometric observations: current status and future plans, Remote Sensing of Environment, 85, 489–506, https://doi.org/10.1016/S0034-4257(03)00051-8, 2003.

Wu, B. and Li, Q.: Crop planting and type proportion method for crop acreage estimation of complex agricultural landscapes, International Journal of Applied Earth Observation and Geoinformation, 16, 101–112, https://doi.org/10.1016/j.jag.2011.12.006, 2012.

Wu, B., Ma, Z., and Yan, N.: Agricultural drought mitigating indices derived from the changes in drought characteristics, Remote Sensing of Environment, 244, 111813, https://doi.org/10.1016/j.rse.2020.111813, 2020.

Yilmaz, M. T., Crow, W. T., Anderson, M. C., and Hain, C.: An objective methodology for merging satellite- and model-based soil moisture products: OBJECTIVELY MERGING SOIL MOISTURE PRODUCTS, Water Resour. Res., 48, https://doi.org/10.1029/2011WR011682, 2012.

Yin, X. G., Jabloun, M., Olesen, J. E., Öztürk, I., Wang, M., and Chen, F.: Effects of climatic factors, drought risk and irrigation requirement on maize yield in the Northeast Farming Region of China, J. Agric. Sci., 154, 1171–1189, https://doi.org/10.1017/S0021859616000150, 2016.

Zeng, J., Li, Z., Chen, Q., Bi, H., Qiu, J., and Zou, P.: Evaluation of remotely sensed and reanalysis soil moisture products over the Tibetan Plateau using in-situ observations, Remote Sensing of Environment, 163, 91–110, https://doi.org/10.1016/j.rse.2015.03.008, 2015.

Zhang, D., Qian, L., Mao, B., Huang, C., Huang, B., and Si, Y.: A Data-Driven Design for Fault Detection of Wind Turbines Using Random Forests and XGboost, IEEE Access, 6, 21020–21031, https://doi.org/10.1109/ACCESS.2018.2818678, 2018.

Zhang, Q., Sun, P., Li, J., Singh, V. P., and Liu, J.: Spatiotemporal properties of droughts and related impacts on agriculture in Xinjiang, China: Spatiotemporal properties of droughts and related impacts, Int. J. Climatol., 35, 1254–1266, https://doi.org/10.1002/joc.4052, 2015.

Zhang, Q., Shi, R., Singh, V. P., Xu, C.-Y., Yu, H., Fan, K., and Wu, Z.: Droughts across China: Drought factors, prediction and impacts, Science of The Total Environment, 803, 150018, https://doi.org/10.1016/j.scitotenv.2021.150018, 2022.

Zhu, X., Li, Y., Li, M., Pan, Y., and Shi, P.: Agricultural irrigation in China, Journal of Soil and Water Conservation, 68, 147A-154A, https://doi.org/10.2489/jswc.68.6.147A, 2013.

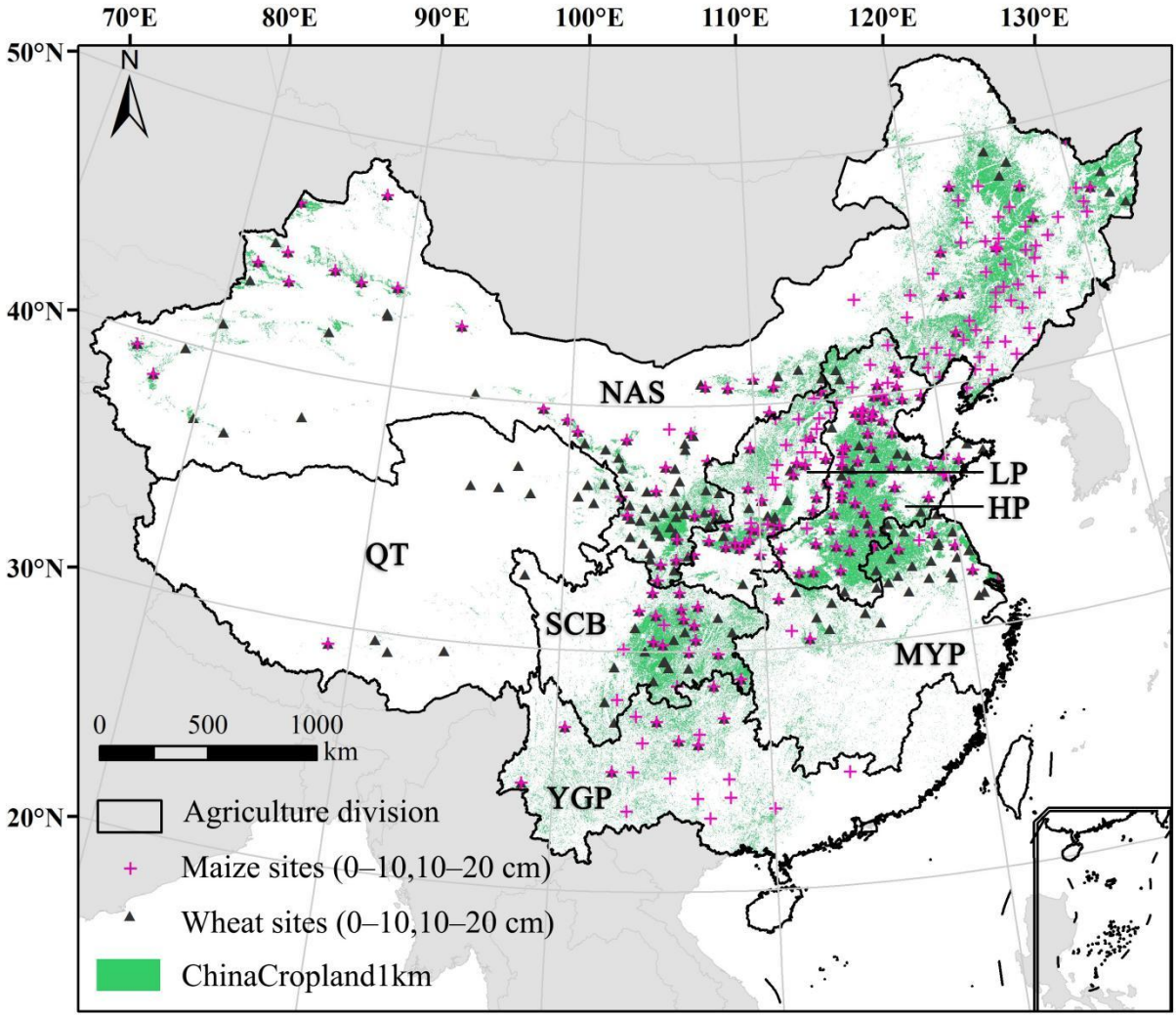

Figure 1 Study areas and the SM in situ field monitoring sites in China. NAS: Northern Arid and Semiarid region; LP: Loess Plateau; HP: Huang–Huai–Hai Plain; SCB: SiChuan Basin; MYP: Middle–lower Yangtze Plain; YGP: Yunnan–Guizhou Plateau and southern China; QT: Qinghai–Tibet region; ChinaCropland1km: the harvesting areas of crops across mainland China.

Table 1 Environmental factors used in the study, including meteorological data (MD), day of year (DOY), classified irrigation (CIR), soil properties (SP), remote sensing data (RSD), and geographical information (GI).

Data type	Variable	Data description	Temporal resolution	Spatial resolution
MD	pre	daily precipitation	daily	1 km
	pre10	ante-accumulated precipitation over ten days	daily	1 km
DOY	DOY	day of year	daily	1 km
CIR	CIR	classified irrigation	-	-
SP	T_REF_BULK	unit: %kg dm^{-3}.	-	1 km
	T_SAND	unit: % wt.	-	1 km
	T_CLAY	unit: % wt.	-	1 km
	T_PH_H2O	unit: %-log (H^+).	-	1 km
	T_GRAVEL	unit: % vol.	-	1 km
	T_SILT	unit: % wt.	-	1 km
RSD	pet	potential evapotranspiration	monthly	4 km
	fc	field capacity	-	250 m
GI	R4	river network vector I	-	-
	R5	river network vector II	-	-
	R12	river network vector III	-	-
	lat	latitude	-	-
	lon	longitude	-	-
	im	moisture index	-	-

Note: REF_BULK: soil bulk density; PH_H2O: hydrogen ion concentration; GRAVEL: volume percentage of crushed stone; T: the topsoil layer. The dash line represents no default values.

Table 2 Evaluation index of relative soil moisture (SMI) in different growth periods of crops at 0–10, 10–20 cm depth.

SMI in different growth periods of wheat (%)								
seeding	seedling	tillering	greening	jointing	booting	grouting	mature	
70~90	75~95			80~95		55~60		
SMI in different growth periods of maize (%)								
seeding	seedling	jointing	booting	tasseling		grouting	mature	
75~85	65~75	70~80	75~85			65~75		

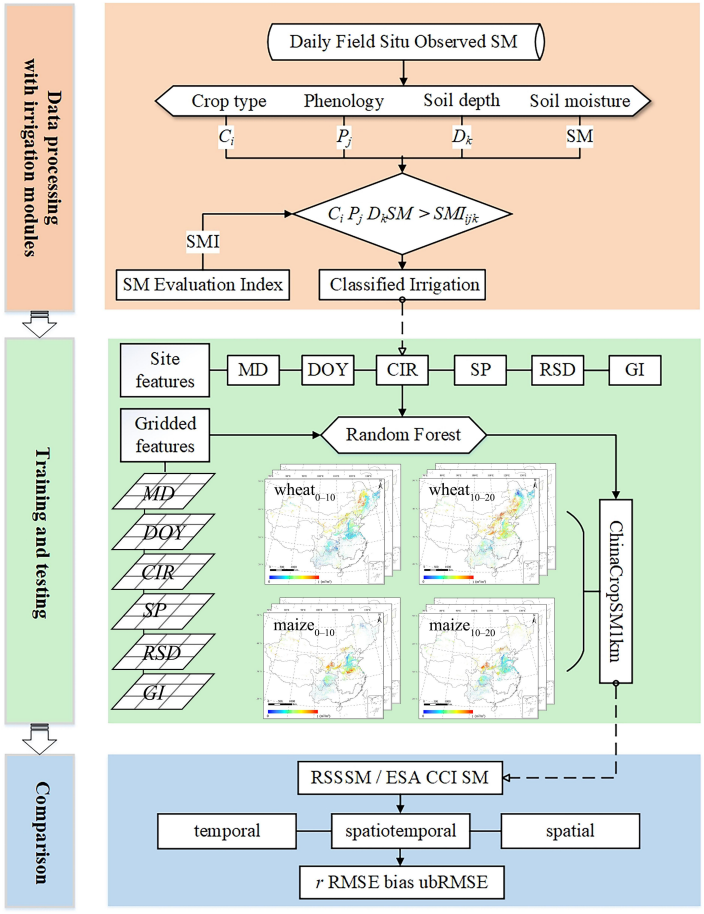

Symbols	Definitions
SM	Soil moisture
C_i	The i th crop type
P_j	The j th phenology
D_k	The k th soil depth
SMI_{ijk}	The soil moisture evaluation index corresponding to the k th soil depth and the j th phenology of i th crop
MD	Meteorological data
DOY	Day of year
CIR	Classified irrigation
SP	Soil properties
GI	Geographical information
RSSSM	The global remote-sensing-based surface soil moisture dataset (2003–2018)
ESA CCI SM	The European Space Agency Climate Change Initiative SM v05.2 (1978–2020)
ChinaCropSM 1km	1-km daily Soil Moisture dataset for Crop drylands across China
maize$_{0-10}$	ChinaCropSM1km for maize harvesting areas at 0–10 cm soil depth
maize$_{10-20}$	ChinaCropSM1km for maize harvesting areas at 10–20 cm soil depth
wheat$_{0-10}$	ChinaCropSM1km for wheat harvesting areas at 0–10 cm soil depth
wheat$_{10-20}$	ChinaCropSM1km for wheat harvesting areas at 10–20 cm soil depth

Figure 2 Flow chart for producing ChinaCropSM1km with an irrigating module.

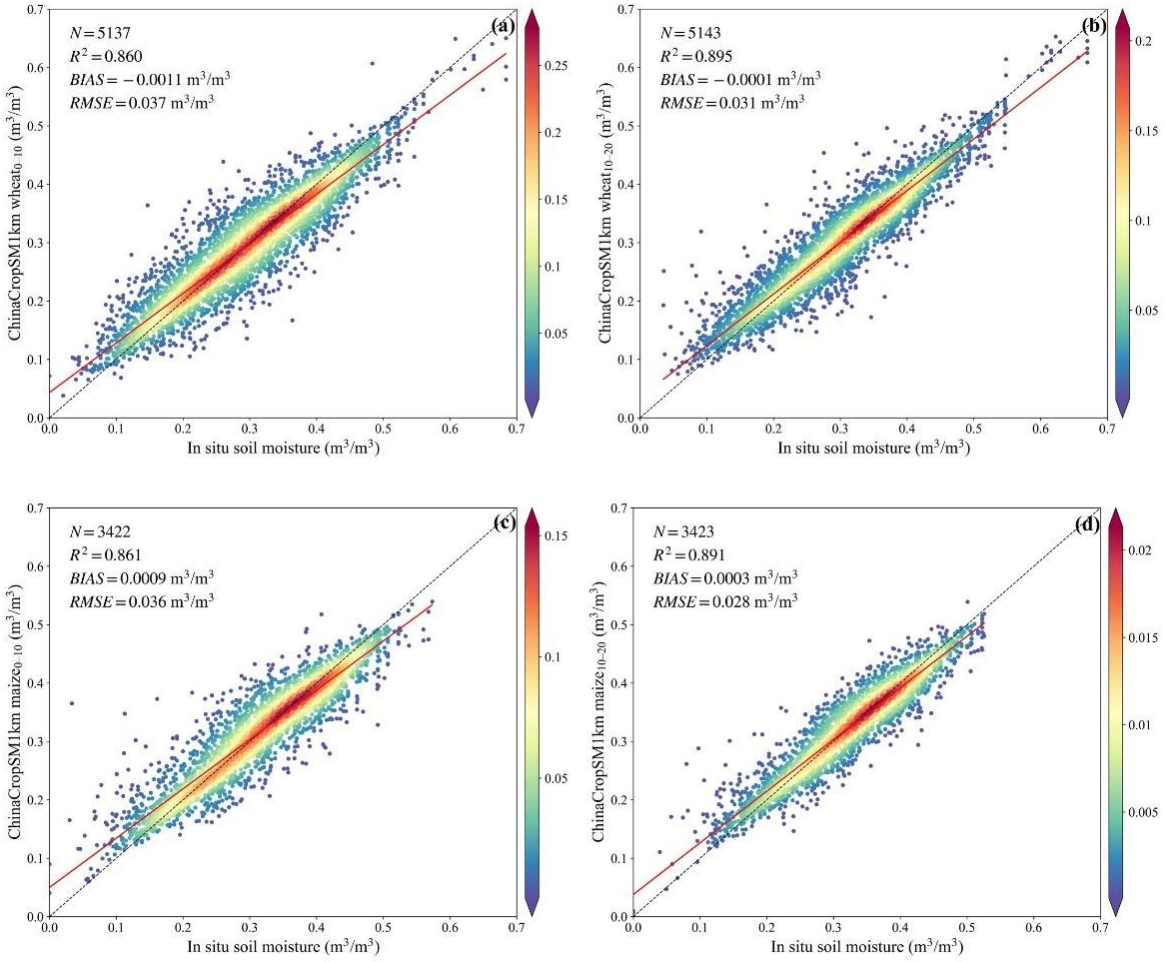

Figure 3 Comparison between the predicted soil moisture (ChinaCropSM1km) and in situ samples by crops and depths (cm). (a) wheat$_{0–10}$, (b) wheat$_{10–20}$, (c) maize$_{0–10}$ and (d) maize$_{10–20}$. The red lines are the trend lines, the colorbar means point density, and the black lines for 1:1 lines.

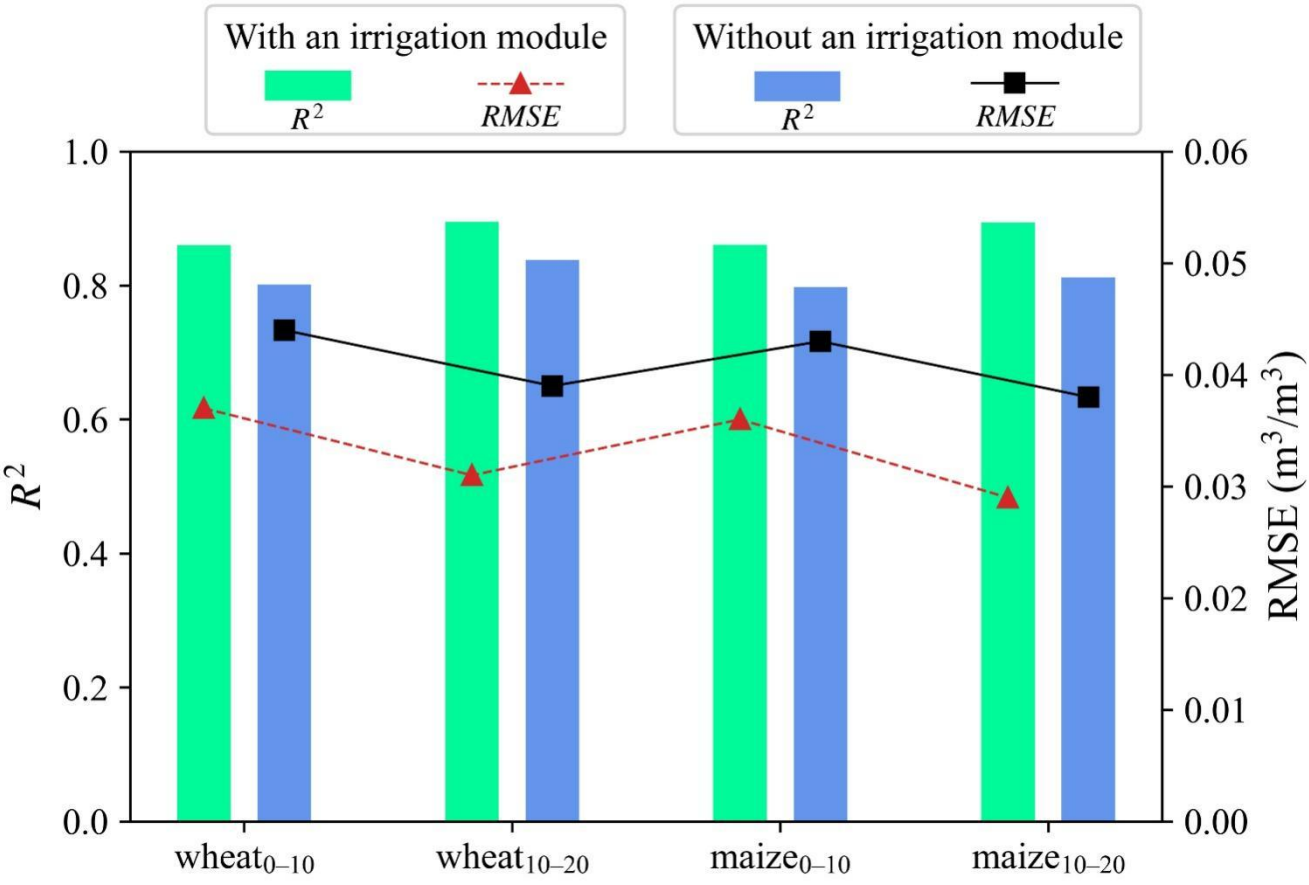

Figure 4. Comparison of soil moisture accuracy between with irrigation and without an irrigation module.

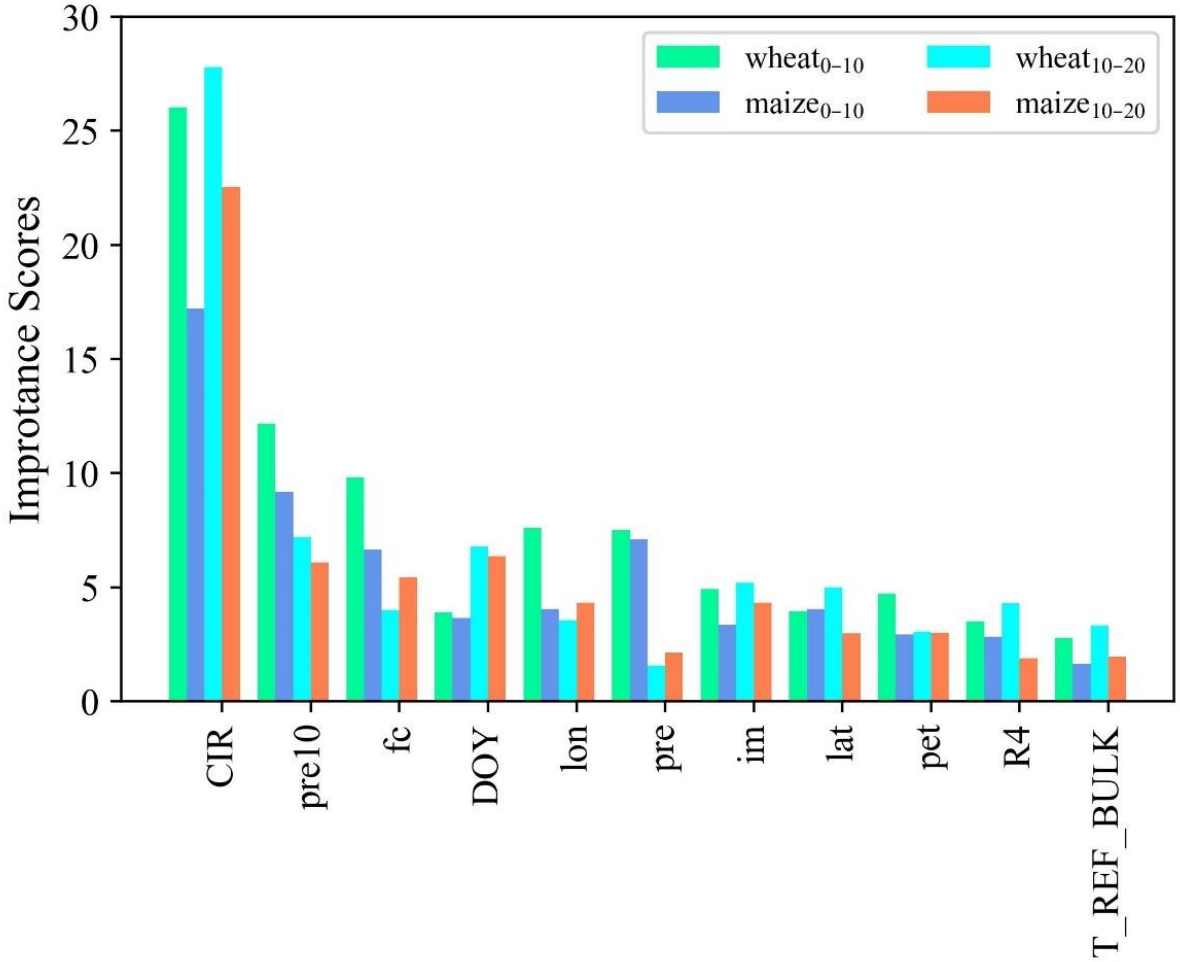

555

Figure 5 The importance scores of 11 independent variables and irrigation factor (CIR).

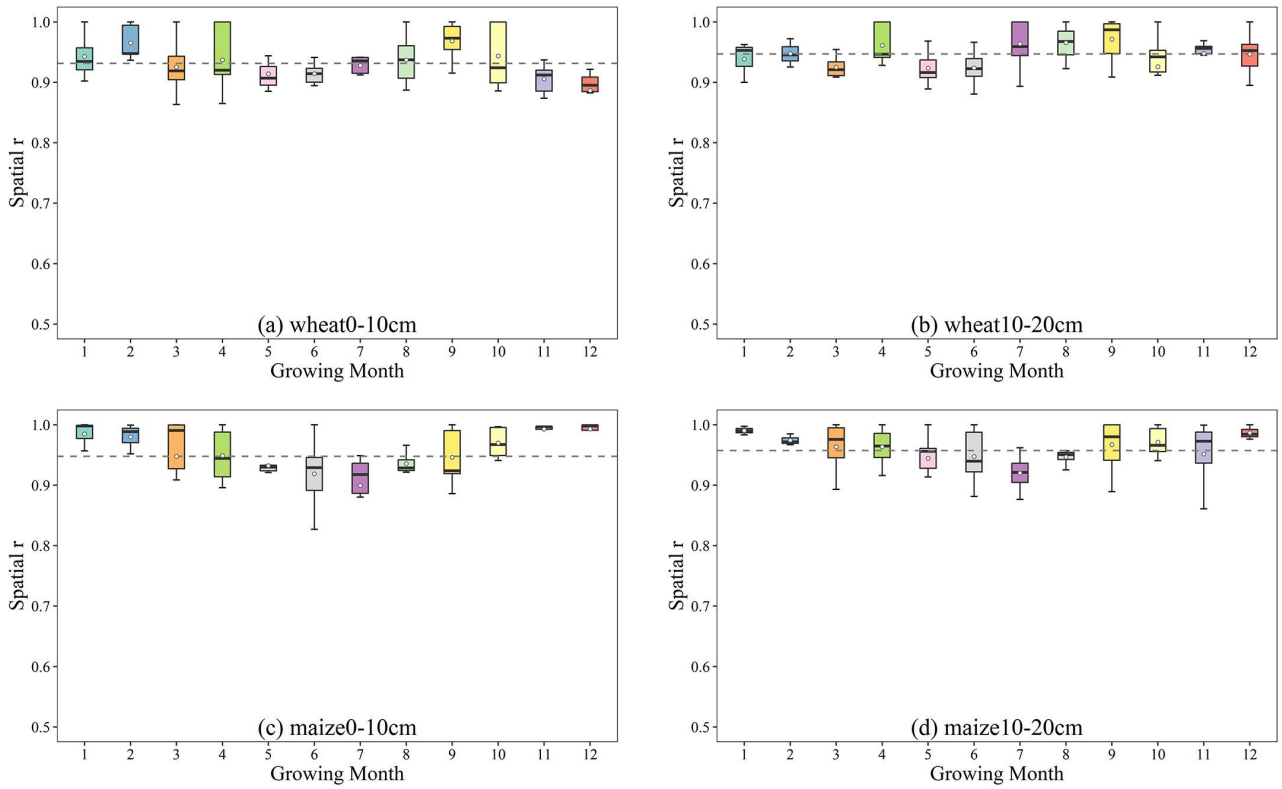

Figure 6 Comparison of the spatial accuracy (*r*) between ChinaCropSM1km and in situ SM observations in each month by crops and depths. (a) wheat$_{0–10}$, (b) wheat$_{10–20}$, (c) maize$_{0–10}$ and (d) maize$_{10–20}$. The dash lines represent the mean values.

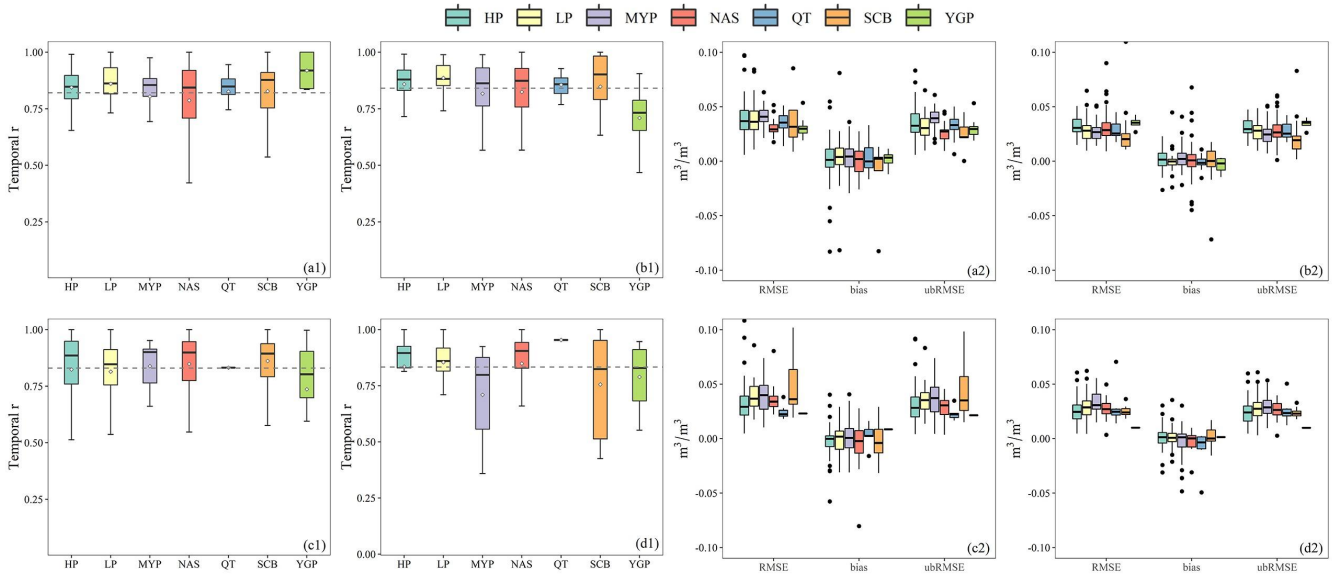

560

Figure 7 Comparison of the temporal accuracy (*r*, RMSE, bias, ubRMSE) between ChinaCropSM1km and in situ soil moisture observations by crops and depths. (a1, a2) wheat$_{0–10}$, (b1, b2) wheat$_{10–20}$, (c1, c2) maize$_{0–10}$ and (d1, d2) maize$_{10–20}$. The dash lines represent the mean values.

Table 3 Summary on means of evaluation indexes (*r*, bias, RMSE, and ubRMSE) of three products (ChinaCropSM1km, RSSSM and ESA CCI SM), all products were compared with in situ surface observations (0–10 cm).

Product	ChinaCrop SM1km$_{maize}$	RSSSM	ESA CCI SM	ChinaCrop SM1km$_{wheat}$	RSSSM	ESA CCI SM
r	**0.93**	0.43	0.35	**0.93**	0.29	0.33
RMSE	**0.033**	0.167	0.126	**0.035**	0.187	0.121
bias	**0.0006**	–0.1361	–0.0846	**–0.0008**	–0.1552	–0.0705
ubRMSE	**0.033**	0.097	0.093	**0.035**	0.105	0.099

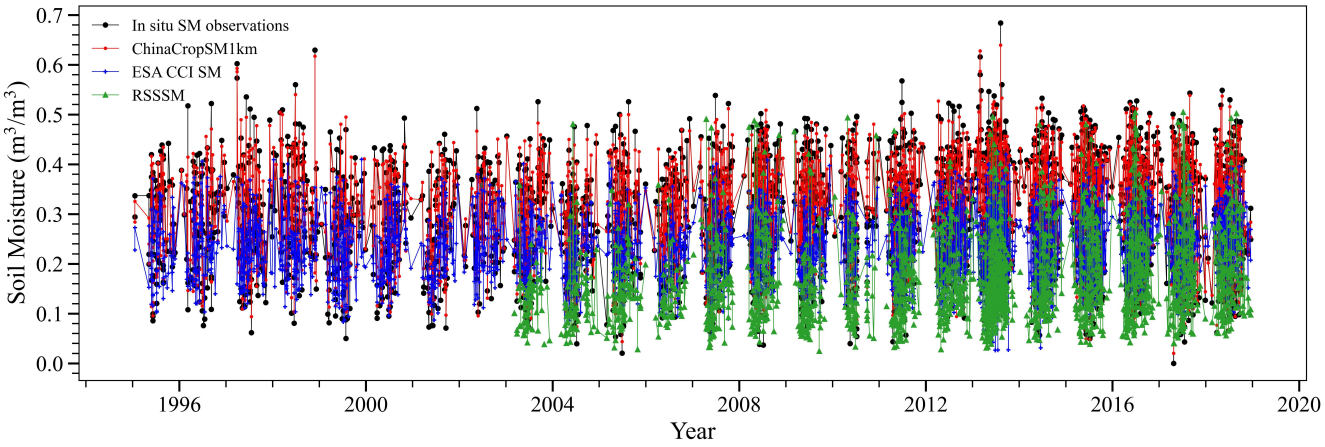

Figure 8 Time series of comparison between in situ SM observations and products.

570

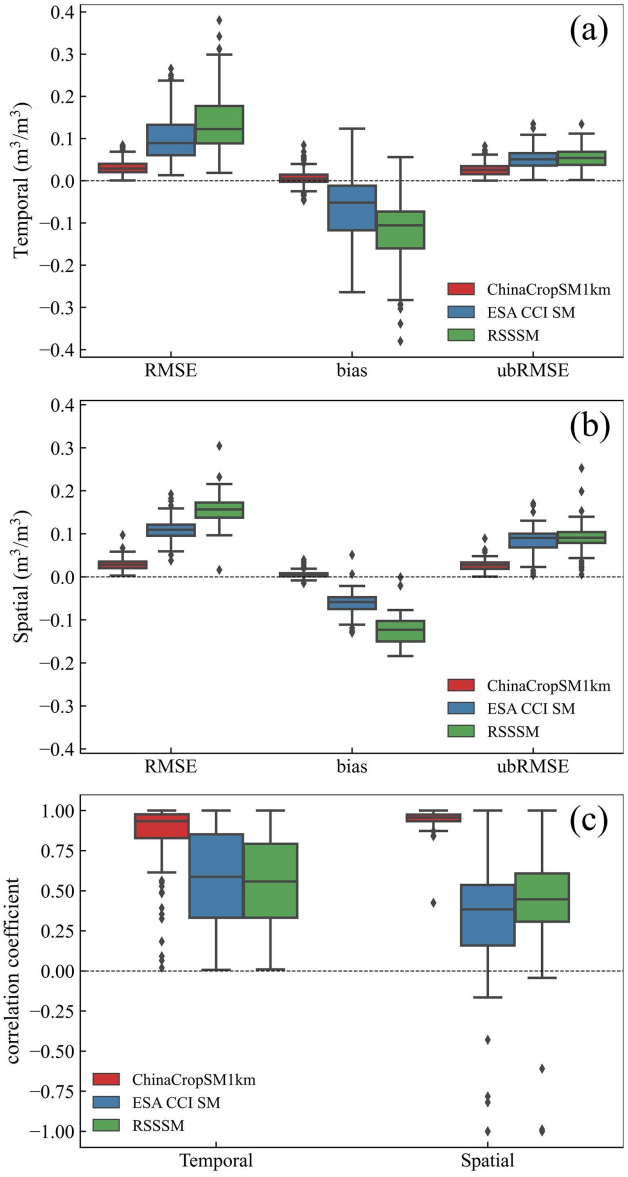

Figure 9 Boxplot of the temporal (a, c) and spatial (b, c) accuracy for ChinaCropSM1km, RSSSM and ESA CCI SM by *r*, bias, RMSE, and ubRMSE. These evaluation indexes were calculated by comparing the three products with in situ SM observations;
575 **the comparison period for ChinaCropSM1km and RSSSM was from 2003 to 2018; and for ChinaCropSM1km and ESA CCI SM was 1995−2018.**